

403072

403 077

CATALOG ACTIA  
AS AD 100

EXPERIMENTAL DETERMINATION OF  
OPEN-LOOP FREQUENCY RESPONSE CHARACTERISTICS  
OF DLG-6 CLASS STEAM GENERATOR SYSTEM

REPORT OF NBTL RDT&E PROJECT B-502-I  
F013-06-06 TASK 4182

4 March 1963

by  
J. W. BANHAM, JR.  
P. H. ZAVOD

**NAVAL BOILER AND TURBINE LABORATORY**  
**PHILADELPHIA NAVAL SHIPYARD**  
**PHILADELPHIA 12, PENNA.**



**EXPERIMENTAL DETERMINATION OF  
OPEN-LOOP FREQUENCY RESPONSE CHARACTERISTICS  
OF DLG-6 CLASS STEAM GENERATOR SYSTEM**

**REPORT OF NBTL RDT&E PROJECT B-502-I  
F013-06-06 TASK 4182**

**4 March 1963**

by  
**J. W. BANHAM, JR.  
P. H. ZAVOD**

---

**APPROVAL INFORMATION**

Submitted by:

  
**J. W. BANHAM, JR.**  
Head, Controls Branch

  
**P. E. JORGENSEN**  
Head, Heat Power Division

Approved by:

  
**W. W. BRALEY**  
Captain, USN  
Director

**REVISED EDITION  
24 April 1963**

TABLE OF CONTENTS

	<u>Page No.</u>
ABSTRACT	i
SUMMARY PAGE	ii
ADMINISTRATIVE INFORMATION	iii
REPORT OF INVESTIGATION	1
Introduction	1
Object	1
Procedure	2
Results	4
1. Automatic Combustion Controls	4
2. Feedwater Regulator	10
3. Forced Draft Blowers	11
4. Main Boiler	13
Conclusions and Discussion	23
1. Automatic Combustion Controls	23
2. Feedwater Regulator	25
3. Forced Draft Blowers	26
4. Main Boiler	
Recommendations	38

## LIST OF ILLUSTRATIONS

<u>Title</u>	<u>Fig. No.</u>
Frequency Response Test Installation	Frontispiece
Bode Diagram - Moore Steam Pressure Controller	1
Steady State Calibration Curve - Fuel Oil Characterizing Relay	2
Bode Diagram - Fuel Oil Characterizing Relay	3
Bode Diagram - Fuel Oil Control Valve	4
Bode Diagram - Forced Draft Blower Actuator	5
Bode Diagram - Air Flow Transmitter	6
Bode Diagram - Copper Tubing	7
Bode Diagram - Feedwater Control Valve	8
Bode Diagram - Hardie-Tynes Forced Draft Blower	9
Steady State Blower Speed vs. Actuator Input	10
Bode Diagram - Steam Pressure/Oil Pressure	11
Transient Response - Superheater Outlet Pressure	12
Bode Diagram - Steam Temperature/Oil Pressure	13
Bode Diagram - Water Level/Oil Flow	14
Transient Response - Water Level/Steam Flow	15
Bode Diagram - Water Level/Water Flow	16
Closed Loop Block Diagram	17

LIST OF ILLUSTRATIONS (Cont'd.)

	<u>Fig. No.</u>
Steady State Calibration Curve-Copes Thermostat	18
Black-Nichols Diagram for Steam Pressure Loop	19
Steady State Steam Temperature vs. Steam Flow	20

ABSTRACT

Open loop frequency response measurements were made of the elements comprising the Foster-Wheeler DLG-6 Class main boiler and its several control loops. Bode diagrams were curve fitted and the approximate transfer functions obtained in mathematical form. Results were analyzed both for agreement of open-loop transfer functions with continuity of energy and mass theory, and for closed loop conformance with stability criteria. Data indicated that steam boiler systems do not lend themselves readily to high performance control, principally due to large phase lags inherent in the process at low frequencies. The chief offenders in this regard are the forced draft blowers, the heat sink, and the additional integrations in the controllers themselves.

SUMMARY PAGE

The Problem:

With the advent of automatic combustion and feedwater control systems and an ever increasing number of applications to naval steam generators, it has become recognized that system designs might be improved of the mathematical nature if the systems were better understood. As a result, the Laboratory has engaged in the experimental determination of the dynamic parameters of several typical naval systems. This report is concerned with the steam generator system for DLG-6 Class..

Findings:

The open loop transfer functions comprising the elements of the DLG-6 boiler, blowers, and controls, were determined from measurement of their frequency response characteristics.

Recommendations:

It is recommended that the results contained herein be made available to the systems industry in the interests of enhancing the state of the art of control system design for naval applications.

ADMINISTRATIVE INFORMATION

Experimental determination of the open-loop dynamic response characteristics of the CVA63, DLG-6, and DLG-9 main boilers and their control systems was authorized by Bureau of Ships letter NP/4 Ser 651A - 993 of 31 July 1961. The research and development project number assigned was F013-06-06, Task Number 4182, and Laboratory Project Number B-502. This is the first of a series of final research project reports.

REPORT OF INVESTIGATION

INTRODUCTION

Experience at the Laboratory and by forces afloat in the operation of automatic combustion and feedwater control systems has indicated that performance of these systems is not always in accordance with specification requirements or designer's intention. Such deficiencies generally result from incompatibility between the control system and the process under control. This problem is not easily overcome in the design stages owing to the lack of suitable information about the dynamics of the process. In an effort to enlarge the store of information relative to dynamic properties of systems in naval engineering plants the Bureau of Ships has authorized the Laboratory to conduct experimental studies to obtain such information. This report covers the investigation and results obtained in one such study, the DLG-6 main boiler, blowers, and automatic controls.

OBJECT

The object of this project was to measure the frequency or transient response characteristics in open loop of the elements comprising the DLG-6 Class main boiler and its accessories, and to express these characteristics mathematically in the form of open-loop transfer functions.

## **NBTL PROJECT B-502-I**

The frequency response technique was to be used for measurement wherever applicable.

### **PROCEDURE**

The Laboratory's DLG-6 boiler installation (NBTL Project B-270) was equipped with instrumentation to provide electrical signals proportional to the following variables:

1. **Combustion and Feedwater Controls**
  - a. Steam pressure controller output
  - b. Air flow controller output
  - c. Selective relay output
  - d. Characterizing relay output
  - e. Feedwater controller output
  - f. Air flow transmitter output
  - g. Steam pressure error
  - h. Air flow error
2. **Boiler**
  - a. Steam flow
  - b. Feedwater flow
  - c. Return fuel oil pressure
  - d. Water level

e. Final steam temperature

f. Superheater outlet pressure

3. Forced Draft Blowers

a. Nozzle valve lifting gear position

b. Forced draft blower speed

An electronic frequency response analyzer, Boonshaft & Fuchs, Inc., Type 711A, was utilized to measure phase and amplitude relationships between sinusoidal variations of pairs of variables as listed above. This device was equipped with an oscillator (adjustable from .01 to 1000 cycles per second) for excitation of the system through an electro-pneumatic converter. The analyzer is designed to compare only the fundamentals at the desired frequencies, rejecting 40 db of all other components; this feature permits a true frequency analysis despite the introduction of non-linear distortions elsewhere in the system. In cases where a frequency response method was not applicable, the open-loop transient response characteristics were obtained by recording responses to step input disturbances using a two-channel recording oscillograph. In cases where the range of interest of frequencies fell below the capabilities of the analyzer, a low frequency oscillator and the recording oscillograph were employed.

Data were obtained by the above techniques and plotted in the form

## NBTL PROJECT B-502-I

of Bode Diagrams. These diagrams were subsequently analyzed to determine the mathematical open-loop transfer functions.

It will be noted that the procedure outlined above produces the perturbed form of the transfer function linearized in a narrow range about the mean operating level. This is not descriptive of the system non-linearities, but does provide a reasonable basis for system design or analysis. The nature and extent of these non-linearities are to be investigated following major revisions to the electronic equipment employed for this type of work.

### RESULTS

The results of this project are shown graphically in Figures 1 through 19. Taken one element at a time, the closed loop system may be described by the following constituent parts:

#### 1. Automatic Combustion Controls

a. Steam pressure controller: This unit, a Moore Products Co. Model 55 Proportional plus Reset stacked diaphragm type controller, was found by its frequency and transient response characteristics to be in unsatisfactory working condition. The Bode diagram for this device, shown in Figure 1, does not conform to the usual proportional plus reset characteristics. The ideal response characteristic curves for this

## NBTL PROJECT B-502-I

instrument are indicated by the solid lines of Figure 1. It is apparent from the experimental data that the reset mode is not present at low frequencies. This of course, is quite the opposite effect of that anticipated, as indicated by the solid-line curves. The ideal curves are located with respect to the gain and frequency scales according to the values of gain and reset time previously determined during control system tests. In an effort to determine the cause of the unusual Bode diagram, the controller was dismantled, inspected, cleaned, and reassembled. Retests produced essentially identical results. A transient response test in which a step change was made in the error signal produced a response curve resembling proportional plus exponential. In service, the unit provided control, but with some proportional offset and insufficient recovery. As an estimate of the performance of a properly adjusted controller, the transfer function shown in Figure 1 was obtained from the idealized Bode curves of Figure 1.

b. Air flow controller: Because of the relatively low natural frequency of this device, a Moore Products Co. Model 68VT17 Proportional plus Reset Controller, it was initially decided to measure the open loop response to a step input to determine the proportional

NBTL PROJECT B-502-I

gain and reset rate. The step changes in the input signal were made in the upward and downward directions with the following results:

Step Increase: Gain = 1.23; Reset rate = .61 rep/min

Step Decrease: Gain = 1.37; Reset rate = .52 rep/min

Dead time = .002 sec

The average transfer function can therefore be expressed as:

$$G(t) = \left[ 1.3 + \frac{.0092}{p} \right] \left[ e^{-.002p} \right]; \quad \frac{\text{psi}}{\text{psi}}$$

It is noted that, in contrast to the steam pressure controller, this device exhibited the customary proportional plus integral transient response. The magnitude of the step changes was 0.7 psi, starting with an initial 9 psi input and output.

The needle valve dial on this instrument indicated a nominal setting of .23 repeats per minute reset rate; the gain is of course non-adjustable and is designed for unity. Indications are that both of these values are substantially in error.

c. Fuel oil burner characterizing relay: This device, General Regulator Co. Model 1771, is designed to convert a controller output representing demand for fuel oil flow per burner to a control valve loading pressure representing demand for fuel oil pressure. Characterizing is done by means of a cam arrangement programmed to

## NBTL PROJECT B-502-1

provide the proper relationship between these functions as dictated by the pressure/flow characteristics of the particular sprayer plates selected for the fuel oil burners. For DLG-6 class, this arbitrary function program of the characterizing relay is illustrated in Figure 2.

The frequency response of the actuator was measured and the resulting Bode Diagram is shown in Figure 3. The solid line indicates experimental values, while the dotted line indicates the approximation obtained by plotting the transfer function shown. The gain scale was located such that zero db represents an amplitude ratio of 2.08 psi/psi, the zero frequency gain measured at the boiler cruising condition. The gain is of course variable with operating level, and can be obtained from the slope of the curve shown in Figure 2 for any average value of input.

The transfer function is of the usual quadratic form associated with the second order response of servo-mechanisms of this type. The transfer function is factorable into two series-connected first order linear lags having time constants of 0.41 and 1.12 seconds. The existence of real roots indicates considerable overdamping. The Bode diagram also approximates a pure second order system with overdamping and a natural frequency of 0.24 cycles per second.

## NBTL PROJECT B-502-I

d. Force-balance fuel oil control valve: This unit responds to the output of the characterizing relay to produce corresponding back pressure in the return fuel oil burner line. It is hydraulically powered by the return fuel oil pressure. Results of frequency response tests, again at the cruising condition, are shown in Bode diagram form in Figure 4. The transfer function is again a factorable lag, with time constants of each component 0.355 and 0.455 seconds. The continued phase shift at higher frequencies indicates that a small amount of backlash exists; the dead time associated with this backlash amounts to 0.023 seconds. The zero frequency gain is 15 db, or 5.6 psi oil pressure per unit psi pneumatic loading pressure.

e. Forced draft blower actuator: The Model 1801 General Regulator Co. pneumatic power actuator positions the throttle linkage of the Hardie-Tynes main forced draft blowers and the combustion control dampers. Frequency response tests were conducted by measuring the angular displacement of the drive crank with respect to sinusoidal variations in the input position demand signal about a fixed reference corresponding to the normal position with two blowers in operation at the cruising condition. The Bode diagram, Figure 5, is a typical second order linear underdamped response. The transfer

## NBTL PROJECT B-502-1

function has the dimensions "degrees rotation per unit psi pneumatic input signal", a natural frequency at .89 cycles per second, and a damping factor of .23. This transfer function is typical of positioning servo-mechanisms of this type.

f. Air flow transmitter: This device, General Regulator Corp. Model 30244, senses the differential air pressure across the burner registers, extracts the square root of this differential pressure and transmits a proportional pneumatic output signal. Frequency response tests were conducted by discharging the output of an electro-pneumatic transducer through a small orifice, and metering the drop across the orifice with the transmitter. Sinusoidal excitation of the e-p transducer thus produces a sinusoidal transmitter output. The orifice differential pressure was related to the corresponding differential across the registers with all burners in use for known values of steady state air flow, thus establishing the zero frequency gain of the transmitter. Data shown in the Bode diagram, Figure 6, illustrate the typical quadratic response of force-balance type instruments.

Curve fitting of the Bode diagram results in very close agreement with the second order transfer function with .50 damping factor. The

## NBTL PROJECT B-502-1

zero frequency gain is measured in cubic feet of air per minute to the boiler furnace, referred to standard conditions. This gain was found to be  $2.41 \times 10^{-4}$  psi output per scfm of air flow to the boiler. The natural frequency of the transmitter was located at 12.6 cycles per second.

g. Copper Tubing: Measurement was made of the frequency response of the 1/4" O. D. copper tubing connecting the ratio relay to one forced draft blower actuator, a distance of approximately 66 feet, with negligible end displacement or capacitance. The Bode diagram, Figure 7, reveals the anticipated fourth order system with natural frequencies of 4.0 and 6.3 cycles per second. It is to be noted that the tubing contributes a gain of nearly 3 db at frequencies in the range of two to three cycles. This may contribute to the high frequency jitter often observed in blower actuators and air flow feedback signals at the control board. The characteristics of other long runs of tubing can be inferred from the experimental results for this particular section.

### 2. Feedwater Regulator

a. Feedwater control valve: The Copes-Vulcan Model CV-D 5" Main Feedwater Regulating Valve was tested by exciting the input to the valve positioner and measuring the response of feed-

## NBTL PROJECT B-502-I

water flow rate while maintaining an average differential pressure across the valve of 75 psi. Results, shown in Figure 8, were very closely approximated by a third order transfer function with backlash. This transfer function consists of a first and a second order component with natural frequencies at .20 and .158 cycles per second respectively. The first order lag is believed to be that of the valve and diaphragm operator, with the time constant associated with the capacitance of the diaphragm chamber; the second order lag is believed to be descriptive of the Moore-Products Co. valve positioner used with the regulating valve. It is noted that considerable underdamping is present, with the result a six db gain at .15 cycles per minute. The third component, .45 seconds of dead time, is attributable to stick-slip friction of the valve stem, probably in the stuffing box. Some of this dead time might be eliminated by installation of fresh packing and proper adjustment of the packing gland.

### 3. Hardie-Tynes Main Forced Draft Blowers.

a. Blower speed/air flow demand: Variation in forced draft blower speed in response to excitation of the actuator input signal are illustrated in Bode diagram form in Figure 9. Response was measured by perturbation of the normal input signal when operating with two

NBTL PROJECT B-502-I

blowers at the cruising condition; combustion control dampers were open under this condition. This response is considered to be grossly non-linear due to characteristics of the steam turbine nozzle valves and the non-linear speed-power relationship. The perturbed form of the transfer function reveals two linear lags, the first associated with the inertial properties of the rotating system, and the second with the compressibility effects of the air at the blower discharge. The zero frequency gain varies with the operating level, and can be obtained from the steady state relationship between speed and actuator input shown in Figure 10. The dynamic non-linearity can be expressed in terms of blower speed; this relationship will be further explored in a subsequent section of the report.

b. Air flow/blower speed : The air flow is directly proportional to the blower speed with all burner registers open, in accordance with steady state fan laws. Considering the dynamic compressibility effects to be included in the speed transfer function, the air flow/speed function can be considered to be pure gain. A plot of blower capacity vs. blower speed produces a linear function with a slope of 4.95 scfm per unit RPM, for one blower. This slope is equivalent to the gain required to express the transfer function obtained

in 2(a) above in terms of air flow per unit air flow demand signal.

#### 4. Main Boiler Energy and Mass Balance.

The energy balance across the boiler under dynamic conditions determines the magnitude of energy stored within the boiler, which in turn fixes the output conditions, pressure and temperature. The open-loop transfer function describing the properties of this heat balance may be listed as follows: steam pressure/heat input, steam pressure/heat output, steam temperature/heat input, steam temperature/heat output, water level/heat input, water level/heat output, water level/water flow, and steam pressure/water flow.

Procedure for obtaining these transfer functions included both transient and frequency response methods. In both cases interactions were avoided insofar as was possible by placing all parameters in open-loop, and measuring responses between output and input pairs. Detailed results were as follows:

a. Steam pressure/heat input: The response of superheater outlet pressure to disturbances in heat input was measured by introducing a sinusoidal oscillation into the fuel rate through the burners while maintaining constant steam, feed, and air flow rates. The system was otherwise permitted to remain in closed-loop and the

## NBTL PROJECT B-502-I

excitation introduced at the set point. Although operation was in closed-loop only the open-loop response was measured. The Bode diagram is shown in Figure 11. Curve fitting yielded a very good agreement with the gain curve, but only a fair approximation of the phase curve. The approximate transfer function was expressed as two series-connected linear lags having widely separated natural frequencies. In general, the high frequency component can be neglected with no appreciable effect on the mathematical description of the system.

The inability to fit the phase curve with accuracy implies that dynamic non-linearities exist. Two principal non-linearities are the heat absorption characteristics of the generating section, and the thermodynamic properties of the steam-water mixture in the boiler. An additional static non-linearity results from the fuel oil burner pressure-flow characteristics. This non-linearity can be eliminated by expressing the input in heat rate or fuel rate terms, as indicated in Figure 11.

b. Steam pressure/heat output: The response of superheater outlet pressure to changes in steam flow was measured by the transient response method. This procedure was necessitated by the fact that the Laboratory's main steam throttle valve is driven by a large induction motor. No means were available for producing oscillatory steam

NBTL PROJECT B-502-I

flow variations, but the high stroke speed available with the motor drive permitted a near step change in valve position. A step change of minus two percent of load was made starting from the cruising steam rate. The response of superheater outlet pressure was recorded. Values of the incomplete response plotted against time on semi-logarithmic paper plotted to nearly a straight line, indicating an exponential, or first order linear lag type response. The single time constant, the value of  $t$  at 36.8 percent incomplete response, was 6.4 seconds. A second component, producing linear decay with time, was identified as an integration. When plotted on rectangular paper as shown in Figure 12, the integration component exhibited a slope of .383 psi/second for a steam flow step change of 4200 lbs/hr. From these data, an approximate transfer function can be derived:

$$P_s = - 1.37 \times 10^{-3} \left( \frac{1}{1 + 6.4p} \right) - .91 \times 10^{-4} \left( \frac{1}{p} \right), \frac{\text{psi}}{\text{lbs/hr}}$$

Where  $P_s$  = Superheater outlet pressure, and  $W_s$  = steam output rate.

c. Steam temperature/heat input: Superheater performance data were obtained by varying the fuel input rate and measuring the superheater outlet temperature response. The steam temperature is a function of the heat absorption in the superheater, which in turn results from conduction, convection, and radiation in the steam generator. Analyzed

## NBTL PROJECT B-502-I

computation of steam temperature by classical heat transfer equations reveals the presence of gross non-linearities in the steady state and transient performance. As is to be expected, this is reflected in the non-linearity of the frequency response characteristics obtained experimentally. The Bode diagram of these characteristics appears in Figure 13; all attempts to curve fit linear equations to these curves to obtain approximate transfer functions were to no avail because of the unusual amplitude-phase relationships. Inspection of Figure 13 discloses large phase lags with increasing frequency accompanied by relatively small reduction of gain. This implies the presence of considerable transport delay time. Transport delay time is of course a common property of heat exchangers; but the high steam velocities in the superheater tubes and piping lend small credence to the existence of substantial amounts of distance-velocity lag between the "center of heat absorption" and the measuring element. On the other hand, if it is assumed that the superheater has a very low heat capacity, then variations in available energy in the gas path can be expected to produce corresponding variations on the steam side. Changes in phase can be attributed to the heat transfer resistance of the steam

## NBTL PROJECT B-502-I

and gas boundary layer films. On this basis it can be argued that the drop in gain with increasing frequency is attributable to the first order lag associated with superheater tube metal heat capacity, and the additional phase shift to several distance-velocity lag components at relatively high, but different frequencies.

d. Steam temperature/heat output: The main steam throttle valve was not capable of sinusoidal oscillation; furthermore, because of the gross non-linearity of the superheater response, as discussed above, it was recognized that results of a transient response test would be essentially meaningless, or at best a very rough approximation. Accordingly, an analytical determination of the response was considered to be more truly descriptive of performance than that to be obtained by any experimental method available. The steady state energy balance across the superheater may be written thus:

$$W_s (h_s - h_g) = K W_o (\text{HHV}) e_b$$

Where:  $W_s$  = Steam flow, lbs/hr

$h_s$  = Enthalpy of superheated steam, Btu/lb

$h_g$  = Enthalpy of saturated steam, Btu/lb

$K$  = Fraction of useful heat absorption from combustion credited to the superheater

NBTL PROJECT B-502-I

$W_o$  = Fuel rate, lbs/hr

HHV = Higher heating value of fuel, Btu/lb

$e_b$  = Boiler efficiency

Substitution of numerical values appropriate to the cruising condition gives:

$$56,000 (1462 - 1183) = K(4130) (18,500)(.878)$$

Solving for  $K$ ,

$$K = \frac{(56,000) (279)}{(4130) (18,500) (.878)} = .23$$

Rewriting,  $W_s (279) = W_o(3740)$

or

$$\frac{W_o}{W_s} = .075$$

It can now be assumed that the Bode diagram of steam temperature/steam flow is identical to that of Figure 13, with the gain scale shifted by a factor of .075, or -22.5 db.

e. Water level/heat input: The frequency response of boiler drum water level with respect to disturbances in heat input was determined by oscillating the fuel oil control valve. A Bode plot of the resulting data is shown in Figure 14. Analysis of the Bode diagram indicated that the transfer function could be closely approximated by two series-connected first-order linear lags, with natural frequencies

NBTL PROJECT B-502-I

at .063 and .279 cycles per second. It is likely that these two components represent the volume displacement changes with respect to heat absorption changes, and mass displacement changes with respect to changes in differential head (hydraulic lag), respectively.

f. Water level/heat output: Response of water level to changes in steam flow were measured by the transient response method, again due to inability to oscillate the steam valve. Step changes in steam flow at the cruising condition, and the resulting variations in water level (holding water flow and oil flow constant) were recorded. The transient response is shown in Figure 15. From these transient response data the transfer function was recognized to consist of two parallel components: a linear lag, and an integration. The first of these is attributable to energy considerations resulting from changes in heat absorption in the generating tubes. This portion of the transient response was further investigated by plotting incomplete response against time on semi-logarithmic paper, and obtaining the time constant at 37.8 percent incomplete response. The average value for the upward and downward step changes was found to be 4.3 seconds. The second component, the integration, results from continuity of mass consideration. A weight rate balance across the boiler indicates that the integration

## NBTL PROJECT B-502-1

results from a difference between steam flow and water flow, and that the integration rate is proportional to this difference and dependent upon the boiler drum geometry. This relationship is further discussed in the following section.

g. Water level/water flow: Sinusoidal variation in feed-water flow about the normal cruising condition was generated by oscillating the main feed regulating valve through a series of test frequencies. The response of water level in the steam drum to these disturbances was measured. The resulting frequency response Bode diagram appears in Figure 16. Analysis of the diagram revealed that the transfer function consisted of two components: a linear lag and an integration, series-connected. Despite the fact that the range of test frequencies was considerably higher than the natural frequency of the low frequency component, it was readily identified as a true integration from the continuity of mass equation, in accordance with the same argument advanced in (f) above.

h. Steam pressure/water flow: Efforts to obtain the response of steam pressure to changes in water flow revealed that the frequencies of interest were well below the capabilities of the frequency response analyzer; attenuation of the steam pressure signal at higher frequencies

NBTL PROJECT B-502-I

produced considerable scatter in the experimental data. The transfer function can, however, be deduced from energy consideration. Consider the energy balance:

$$h_f + \Delta h_f = \frac{K \int (K_1 W_o - K_2 W_s + K_3 W_w + K_3 \Delta W_w) dt}{W_m + \Delta W_m}$$

Where:  $h_f$  = change in enthalpy of saturated liquid, Btu/lb

$W_o$  = Fuel rate, lbs/hr

$W_s$  = Steam rate, lbs/hr

$W_w$  = Water rate, lbs/hr

$W_m$  = Weight of water/steam mixture in the boiler, lbs

$K$  = Constant

The first three terms in the integral represent steady state conditions, and their sum must be equal to zero. The value of the integral when divided by the weight of the contents of the steam generating system is a measure of the unit energy of the boiler mixture and roughly equal to the enthalpy of the saturated liquid at the operating pressure. For a small perturbation in water flow the weight of boiler contents can be considered constant. Therefore the equation can be rewritten:

$$\Delta h_f = \frac{K}{W_m} \int (K_3 \cdot \Delta W_w) dt$$

In view of the fact that the saturated liquid enthalpy varies linearly with pressure in the range of operating pressures under consideration, the above may be expressed as:

$$\Delta P_s = \left( \frac{\Delta P_s}{\Delta h_f} \right) \left( \frac{K K_3}{W_{fm}} \right) \left( \Delta W_w \right) dt$$

Or in transfer function form:

$$P_s / W_w = 2 \pi f_n \left( \frac{1}{p} \right)$$

The same analysis may be applied to the steam flow and fuel flow terms of the basic equation. The natural frequency in each case is a function of boiler geometry, capacity, circulation and heat absorption characteristics, and operating pressure. Transfer functions for steam flow or feedwater flow are related by the ratio of  $K_3$  to  $K_2$ , which in turn are proportional to the heat absorption in boiling and in pre-heating to saturation. At the cruising condition:

$$\frac{K_3}{K_2} = - \left( \frac{h_f - h_{econ}}{h_{fg}} \right) = \frac{215-366}{608} = 0.25$$

and 
$$\begin{matrix} (f_n) & = & .25 (f_n) \\ \text{feedwater} & & \text{steam} \\ \text{flow} & & \text{flow} \end{matrix}$$

From the integration term of the steam pressure/steam flow

transfer function of Figure 12, the transfer function being sought (neglecting low frequency effects) is:

$$\frac{P_{s_w}}{W_w} = - .25 \times .91 \times 10^{-4} \left( \frac{1}{p} \right), \text{ or}$$

$$\frac{P_{s_w}}{W_w} = - .228 \times 10^{-4} \left( \frac{1}{p} \right), \frac{\text{psi}}{\text{lbs/hr}}$$

This transfer function is analytically derived, but based on the experimentally determined value of the natural frequency of a related function.

#### CONCLUSIONS AND DISCUSSION

Conclusions pertaining to results previously described are in corresponding order:

##### 1. Automatic Combustion Controls:

a. The steam pressure controller did not exhibit the anticipated proportional plus reset characteristics, thus explaining subsequent marginal performance of the control system when operating in closed loop. Inspection of this component failed to disclose the reason for its unusual characteristic response. In general, it has been the Laboratory's experience that the stack diaphragm type controllers, particularly those employing pressure-splitting gain circuitry exhibit

**NBTL PROJECT B-502-I**

troublesome unreliable performance. In any case, no credence should be given to the dial readings of calibrated needle valves used in instruments of this type.

b. Air flow controller transient response conformed to anticipated, in contrast to that of the steam pressure controller. Non-linearity of this device was revealed in the varying gain and reset rate values obtained under increasing and decreasing step input conditions. Again the reset rate needle valve dial did not agree with the measured reset value.

c. The fuel oil characterizing relay is essentially a pneumatic force-balance servo-mechanism. The quadratic lag measured in frequency response tests was considered typical of devices of this type.

d. The fuel oil control valve also exhibited a characteristic quadratic lag with considerable overdamping. It is interesting to note that this device has a better frequency response than the characterizing relay which drives into it.

e. The response of the forced draft blower pneumatic throttle actuator was considered typical of the characteristics of units of this type.

## NBTL PROJECT B-502-I

f. The response of the air flow transmitter was again a typical second order function usually associated with force-balance instruments.

g. The characteristic Bode diagram for copper tubing was of a form coincidental with published results of other investigations. The analysis of the dynamics of transmission lines is extremely complex and is generally considered too complicated for practical engineering applications. Assuming that the receiver volume remain small in relation to the volume of the tubing, use of an inverse proportion relationship between tubing length and natural frequency for each of the quadratic terms will provide a useful approximation. The transfer function indicated in Figure 7 is for a section of dead ended tubing, 66 feet in length. Other transmission lines of roughly equal lengths are found at the output of the air flow transmitter and steam pressure transmitter.

### 2. Feedwater Regulator

a. The feedwater control valve characteristics conform closely to a second order lag with additional first order and backlash components representative of diaphragm chamber capacity and friction. The backlash dead time of one half second is believed to be excessive, but fortunately does not appear to introduce excessive phase shift in the

closed loop. This backlash might be relieved by packing, lubrication, or similar maintenance.

### 3. Main Forced Draft Blowers.

a. The Bode diagram of Figure 9 illustrates the perturbed frequency response of one blower operating at the two-blower cruising condition. Recognizing that the transfer function is non-linear, the experimental results may be compared to analytical results as follows: The angular acceleration of the blower rotor is directly proportional to the net applied torque, and inversely proportional to the polar moment of inertia. Hence:

$$\frac{d\omega}{dt} = \frac{1}{MK^2} \cdot (T_1 - T_2)$$

Where:  $\omega$  = Angular velocity

M = Mass of rotating system

K = Radius of gyration

T<sub>1</sub> = Torque applied by turbine

T<sub>2</sub> = Torque applied by fan

In terms of revolutions per minute and polar moment of inertia, and integrating:

$$N = \frac{K}{I_p} (T_1 - T_2) \left( \frac{1}{p} \right)$$

NBTL PROJECT B-502-I

Where:  $N$  = Angular velocity, RPM

$I_p$  = Polar moment of inertia

$K$  = Constant

$p$  = Differential operator,  $\frac{d}{dt}$

The torque applied by the fan acts as a brake; this torque varies directly with the square of angular velocity. Therefore:

$$\frac{2\pi}{60} N = \frac{1}{I_p} (T_1 - CN^2) \frac{1}{p}$$

and 
$$\frac{N}{T_1} = K_1 \left( 1 - \frac{CN^2}{T_1} \right) \frac{1}{p}$$

This equation is the transfer function of the response of blower speed to changes in applied torque. In perturbed form the applied torque can be considered proportional to steam flow, and the braking torque proportional to rotational speed.

$$\frac{2\pi}{60} N = \frac{1}{I_p} (C_1 W_s - C_2 N) \frac{1}{p}$$

$$\left( \frac{2\pi I_p}{60} \right) N = C_1 W_s \left( \frac{1}{p} \right) - C_2 N \left( \frac{1}{p} \right)$$

$$\left( \frac{2\pi I_p}{60} \right) N \left( 1 + \frac{60 C_2}{2\pi I_p} \right) = C_1 W_s \frac{1}{p}$$

$$\frac{N}{W_s} = \frac{60 C_1 (1/p)}{2\pi I_p \left( 1 + \frac{60 C_2}{2\pi I_p} \cdot \frac{1}{p} \right)}$$

$$= \frac{9.55 C_1}{I_p (p + 9.55 \frac{C_2}{I_p})} = \frac{C_1/C_2}{(1 + .1047 (\frac{C_2}{I_p}) p)}$$

The transfer function now appears in first order linear lag form,

where:

$N$  = Rotational speed, RPM

$W_s$  = Steam flow to turbine

$C_1$  = Slope of torque/steam flow curve

$C_2$  = Slope of torque/speed curve

The time constant has the value  $.1047 I_p/C_2$ , indicating that rapid dynamic response can be expected of blower designs having minimum polar moments of inertia and maximum rate of change of torque with respect to angular velocity. The transfer function derived above constitutes the principal dynamic lag in the response of the forced draft blower, and is equivalent to the lower frequency lag components of the experimentally determined transfer function shown in Figure 9. The higher frequency component probably arises from the resistance and

## NBTL PROJECT B-502-I

capacitance at the blower discharge. This RC network will result in a phase lag between speed and air flow, which will produce a corresponding lag between speed and static pressure, hence speed and power, hence speed and retarding torque. Because of the complex system geometry the numerical value of this capacitance is difficult to compute with any degree of accuracy. In general it appears that rapid dynamic response can be further promoted by boiler designs which minimize draft losses and air and gas side volume.

The backlash term, a relatively high frequency component, is caused by the mechanical lost motion in the blower throttle valve linkage.

b. As discussed in the Results section, the air flow/blower speed transfer function can be considered a proportional conversion if the attenuation and phase shift resulting from compressibility effects are assigned to the blower transfer function. In order to complete a closed loop description of the system units of the transfer function must be expressed in terms of degrees rotation of the throttle linkage, and the appropriate dimensions associated with actuator displacement included. This breakdown is shown in the block diagram of Figure 17.

4. Transfer functions for the main boiler energy and mass relationships are discussed in the same order as presented in the previous

section, Results.

a. The steam pressure/heat input transfer function for the boiler can be applied to steam pressure at either the superheater outlet or at the steam drum, since the pressure changes are small and the steam flow was constant. According to heat balance considerations the Bode diagram should indicate a response characteristic of pure integration. As illustrated in Figure 11, however, the transfer function was found to consist principally of a first order lag with low natural frequency. The discrepancy is resolved with the recognition that the enthalpy of saturated steam is not constant with the saturation pressure. An increase in saturation pressure required additional heat absorption to maintain equilibrium. This constitutes a form of negative feedback in the integration loop, which converts the integration to a first order lag.

A further consideration is the effect of steam pressure changes in the steam output. During test runs the steam valve and all other restrictions in the steam piping constitute a fixed system resistance. Pressure changes therefore, produce steam flow changes in accordance with critical flow considerations wherein steam flow varies directly with absolute steam pressure.

By the same argument, variations in heat input produce corresponding variations in steam temperature with the result an added

variation in heat output.

Attempts to modulate steam flow to maintain constant heat output are considered highly impractical. The transfer function therefore includes all three of the aforementioned effects.

b. The transient response of steam pressure to heat output is shown in Figure 12. This response appears to contain two parallel connected transfer functions, a first order lag, and an integration. In the light of the discussion in (a) above, it seems difficult to justify the existence of the integration term. Apparently the transient response was not carried to ultimate completion, with the result the loss of low frequency data which might otherwise have revealed the presence of a linear lag in lieu of a pure integration. On the other hand, the integration is in accordance with the theory, the exponential characteristics being explained by the side effects described in (a) above. If we assign the dimensions steam pressure/heat input and steam pressure/heat output to these two transfer functions, only the higher frequency responses should be considered. In any case, these two functions should be compatible in form. With this in mind, and neglecting feedback effects, the steam pressure/heat input transfer function can be modified to yield the following:

$$\frac{P}{W_0} = 15 \times 10^{-4} \left( \frac{1}{p} \right) \left( \frac{1}{1 + .4p} \right), \frac{\text{psi}}{\text{lbs/hr}}$$

c. Steam temperature characteristics of the superheater were adequately determined by experimental frequency response techniques. Unfortunately, no linear analytical transfer function could be found to approximate the experimental data. On the other hand, this response does not constitute an element of the closed loop system, and is therefore of less analytical importance. The Bode diagram of Figure 13 may be useful in establishing criteria for superheater designs under adverse transients or thermal fatigue conditions, for temperature transmitter or indicator design, etc.

d. The Bode plot for response of steam temperature to steam flow may be obtained by shifting the amplitude curve of Figure 13 down 71.5 db, as discussed under paragraph 3 d of "Results".

e. Boiler drum water level response to changes in fuel rate are indicated in Figure 14. This response takes the form of two series-connected first order lags. This effect is analogous to the "shrink and swell" phenomenon commonly observed as response to changes in steam rate.

f. Water level/heat output, or more properly, water level/steam flow, was determined by transient response methods. In addition, to the linear lag representing shrink and swell, the integration

NBTL PROJECT B-502-I

term observed was a measure of the loss (or gain) of weight of contents of the boiler due to differences between input and output flow rates. In terms of drum water level, the rate of integration (as determined from the transient response curve of Figure 15) was  $-1.15 \times 10^{-6}$  inches per second per pound per hour steam flow/water flow differential.

g. The water level/water flow transfer function obtained from the frequency response results shown in Figure 16 exhibited a low natural frequency integration as the primary component. This integration results from the mass continuity equation, and in theory is the complement of the water level/steam flow integration discussed in (f) above. The natural frequency of this function occurs where the gain is unity (zero db), and from the natural frequency the integration rate,  $2\pi f_n$ , was found to be  $1.13 \times 10^{-6}$  inches per second per pound per hour steam flow/water flow differential. Considering the fact that the steam flow and water flow effects on boiler water level were obtained by different methods, using different instrumentation, and in separate test runs, the close agreement between these complementary functions is considered nothing less than remarkable.

h. The steam pressure/water flow transfer function was derived analytically and the natural frequency based on other experimental

NBTL PROJECT B-502-I

results. This analysis appears in paragraph 3(h) of "Results". Further experimental justification for the transfer function obtained is contained in the following section.

5. The closed loop block diagram appears in Figure 17. Consideration of the elements comprising this diagram gives rise to the following:

a. The energy balance across the boiler indicates that all integration components in the heat balance transfer functions must add to zero at steady state steaming conditions. Based on a steaming rate of 56,000 pounds per hour, with fuel rate 4200 pounds per hour, the natural frequencies of the transfer functions of Figures 11 and 12 and paragraph 3(g) of "Results" can be converted to Btu's and algebraically summed as follows:

$$\left( \frac{f_{np}}{W_s} \right) (W_s) = -.91 \times 10^{-4} \times 56,000 = -5.10$$

$$\left( \frac{f_{np}}{W_w} \right) (W_w) = -.228 \times 10^{-4} \times 56,000 = -1.28$$

$$\left( \frac{f_{np}}{W_o} \right) (W_o) = 15.0 \times 10^{-4} \times 4200 = +6.30$$

The algebraic sum,  $-.08$ , represents an experimental error of  $(.08/6.38)$ , or about 1.25 percent. This error is considered within

the limitations of test instrumentation and technique. This level of accuracy further justifies the analytical transfer function obtained in paragraph 3 (h) of "Results".

b. The mass balance across the boiler also requires that all integration components add to zero at steady state. Thus the natural frequencies of the water level/steam flow and water level/water flow transfer functions from Figures 15 and 16 may be summed as follows:

$$2\pi(f_n)_{w/s} = -1.15 \times 10^{-6}$$

$$2\pi(f_n)_{w/w} = 1.13 \times 10^{-6}$$

The algebraic sum,  $-.02 \times 10^{-6}$ , reflects an experimental error of about 1.8%, a remarkably high degree of experimental accuracy.

c. Several of the elements comprising the closed loop systems shown in Figure 17 were not evaluated. These elements include the Copes-Vulcan feedwater control system, including the thermo-mechanical transmitter; the Bailey KP-13 steam pressure transmitter; the General Regulator ratio relays; and the General Regulator low pressure signal selector. In the case of the transmitters the inputs could not be independently controlled; in the case of the mechanical combining relay of the feedwater regulator the three

## NBTL PROJECT B-502-I

element inputs could not be simulated in open-loop; the ratio relays were considered to have flat frequency responses in the range of interest, and were therefore gain devices only; the low pressure signal selector is essentially a binary logic device, and its frequency response is not descriptive of its function in an analog loop.

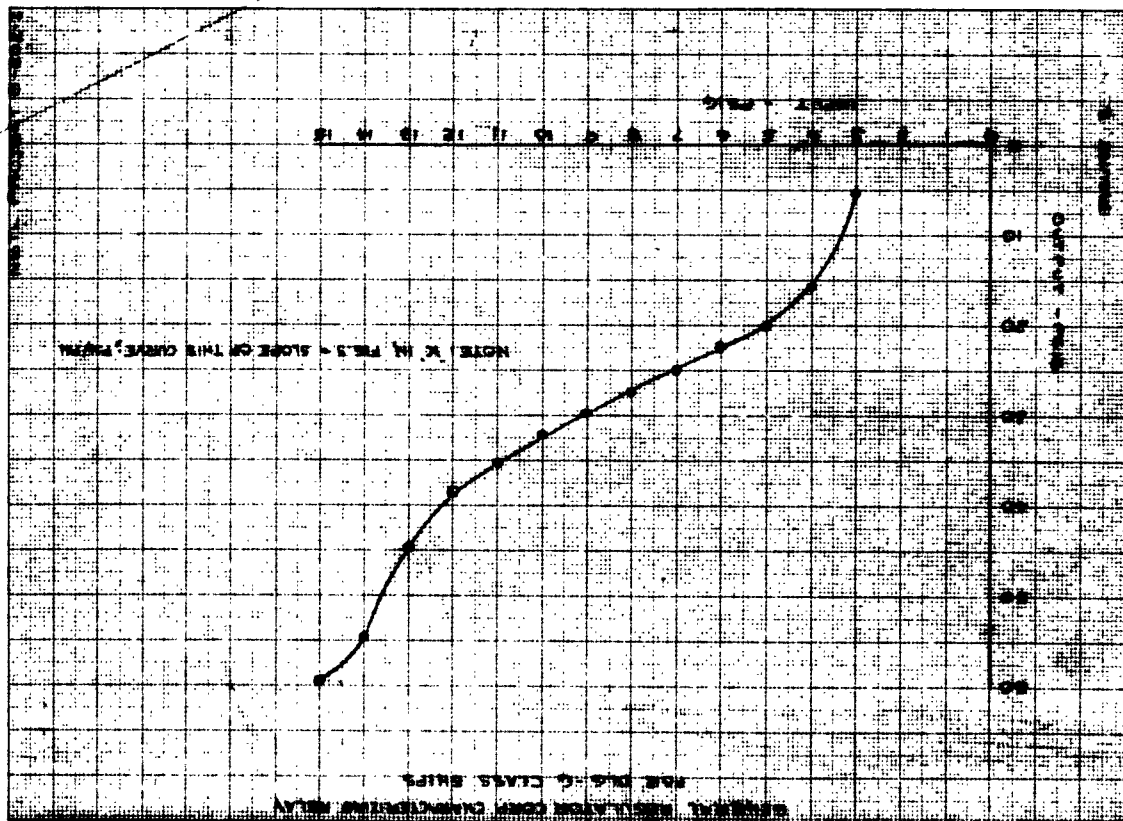
The only devices listed above that contain static non-linearities are the feedwater regulator components. The thermostat output as a function of water level in the boiler drum is shown in Figure 18; the flow elements of the combining relay produce inputs to the controller that vary with the square root of the flows. These functions are included in the block diagram, Figure 17.

d. The closed loop frequency response can be obtained from a Black-Nichols plot of the open loop frequency response of the system. Such a diagram appears in Figure 19. This diagram represents the response of the closed loop to disturbances in the set point steam pressure. From the Black-Nichols diagram it is evident that the maximum gain of the closed loop is 9 db, occurring at a frequency of .004 cycles per second. The closed loop phase angle is  $-60^{\circ}$ . The closed loop diagram indicates that stability criteria are not being met. Response to an increase in set point indicates

**NBTL PROJECT B-502-I**

excessive low frequency phase shift, that to a decrease in set point, insufficient loop gain.. These two conditions bracket the ideal closed loop gain and phase stability criteria, indicating that the system is optimally adjusted while at the same time inherently incapable of optimum performance. These conclusions are supported by observation of control system performance on the Laboratory boiler. From the diagram it is further obvious that one method for improvement of the system response lies in elimination of the reset mode in the steam pressure control loop. This in fact is exactly the technique employed in the systems for DD945 and DLG-9 Class.





100-1000-1000  
 100-1000-1000  
 100-1000-1000

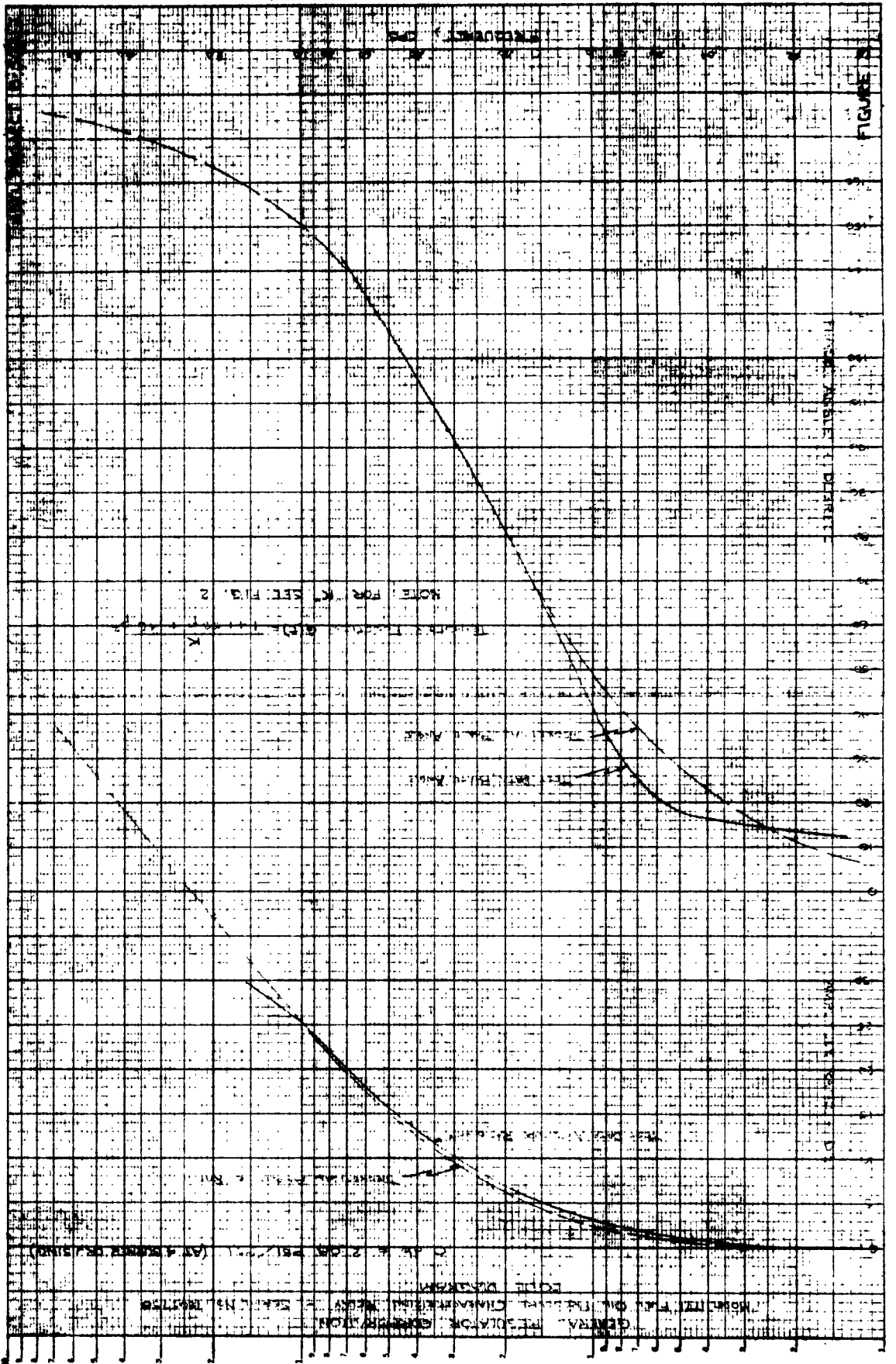


FIGURE 2

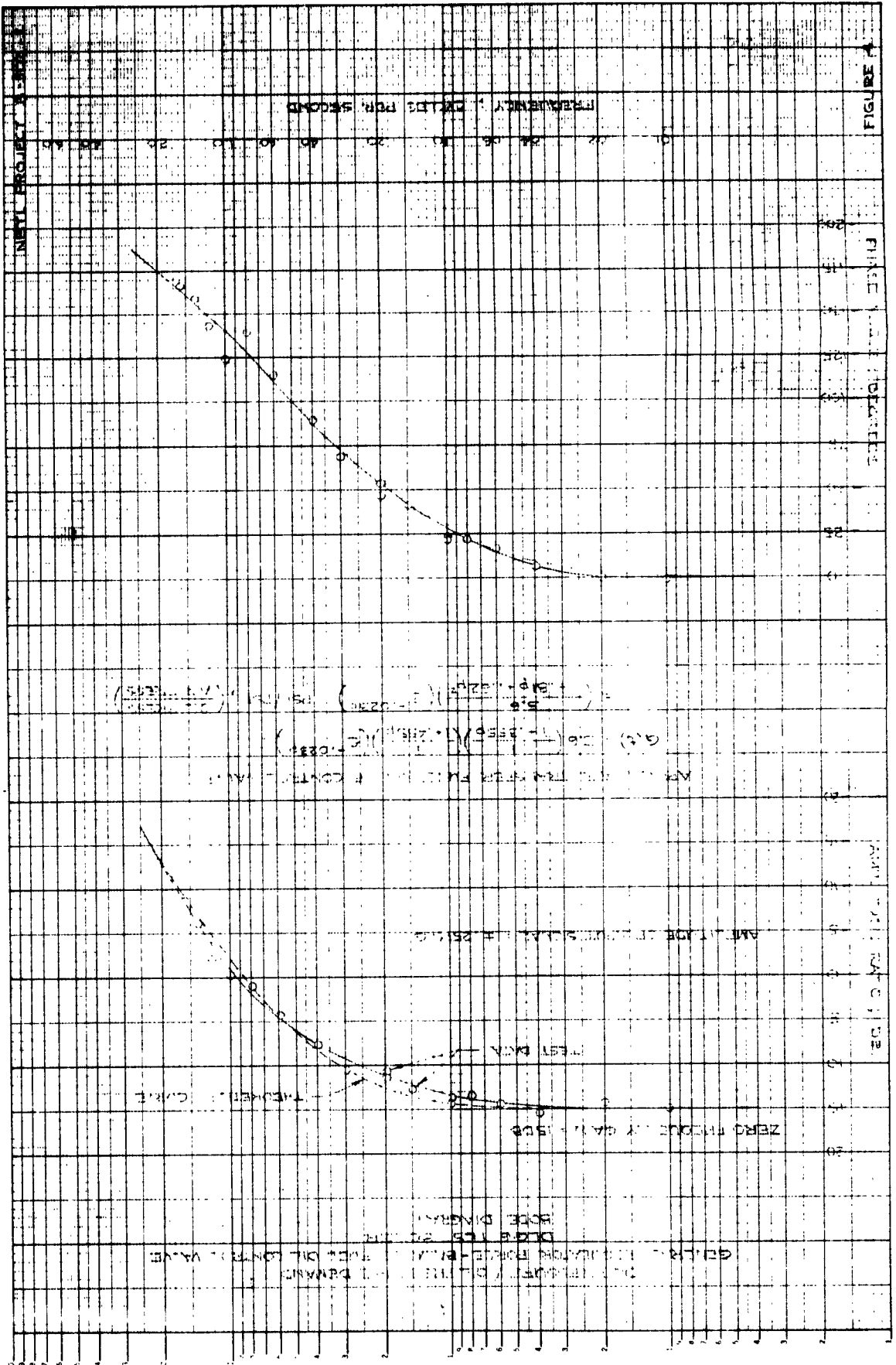
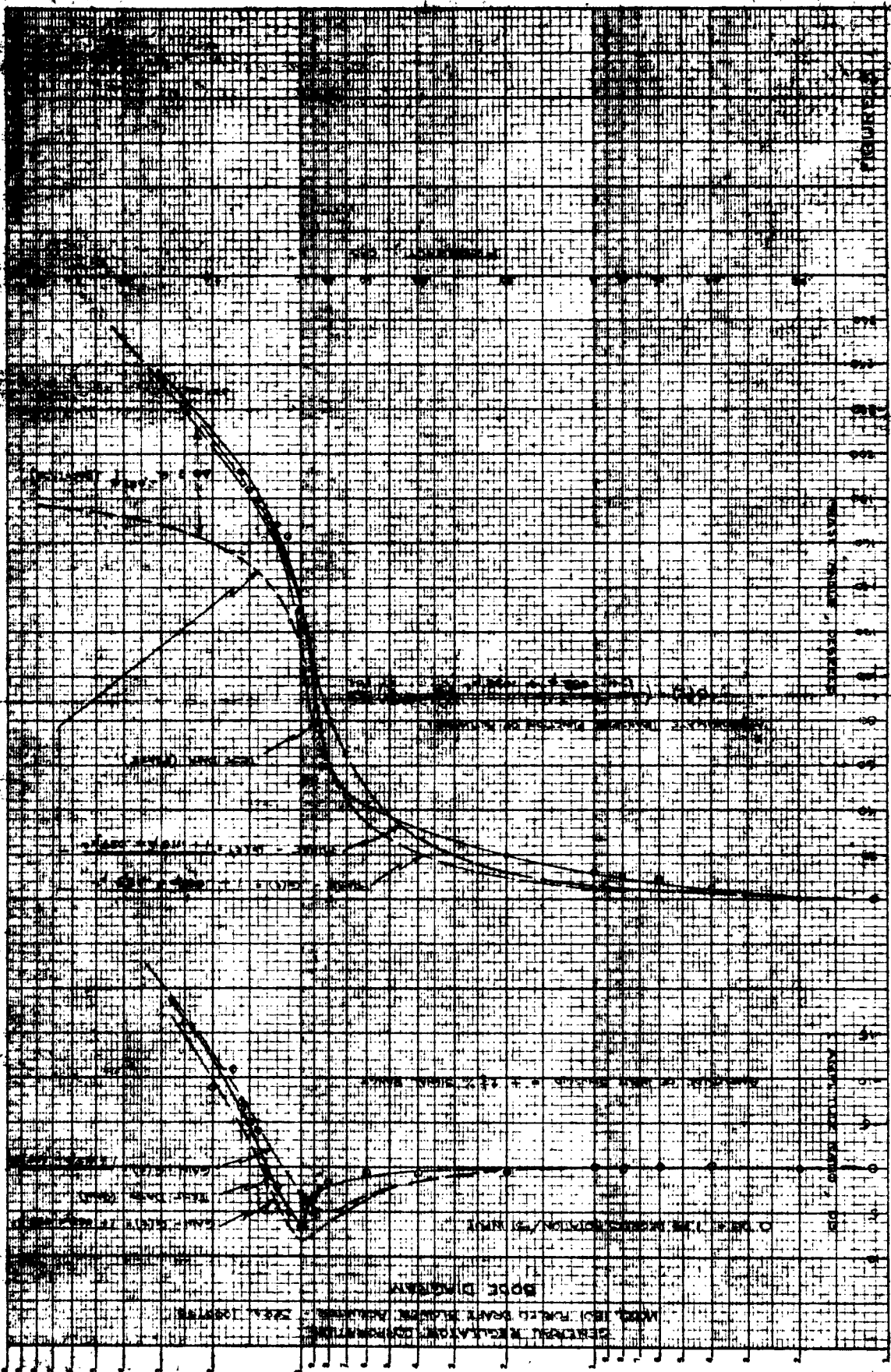


FIGURE 4



K-E SEMI-LOGARITHMIC 380-7110  
 SUPPORT & RANGE 2 100 DIV. 100  
 1000 100 10 1

GENERAL ELECTRIC COMPANY  
 MODEL 100 PORTABLE SCANNER  
 BOSTON, MASSACHUSETTS

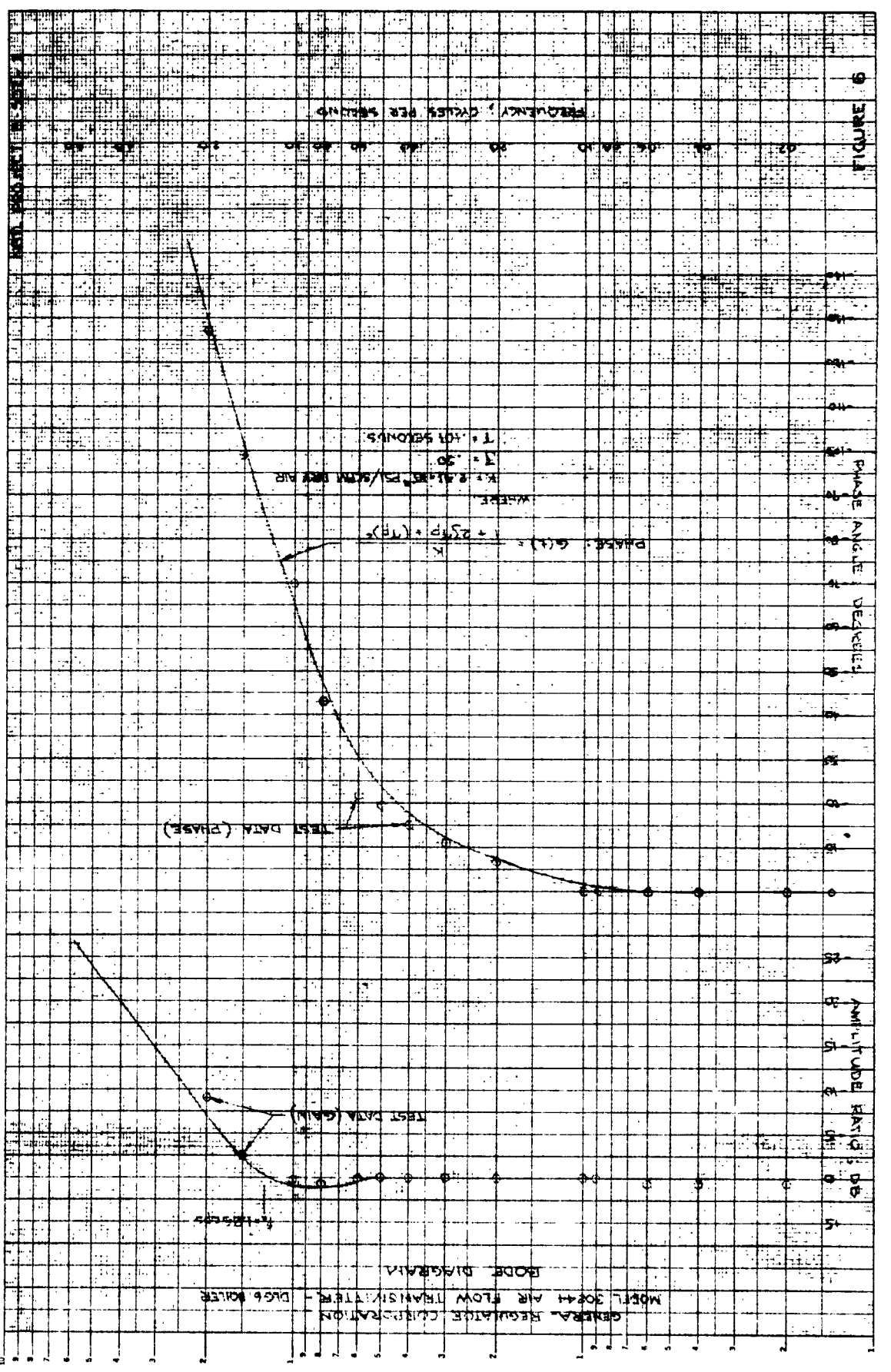
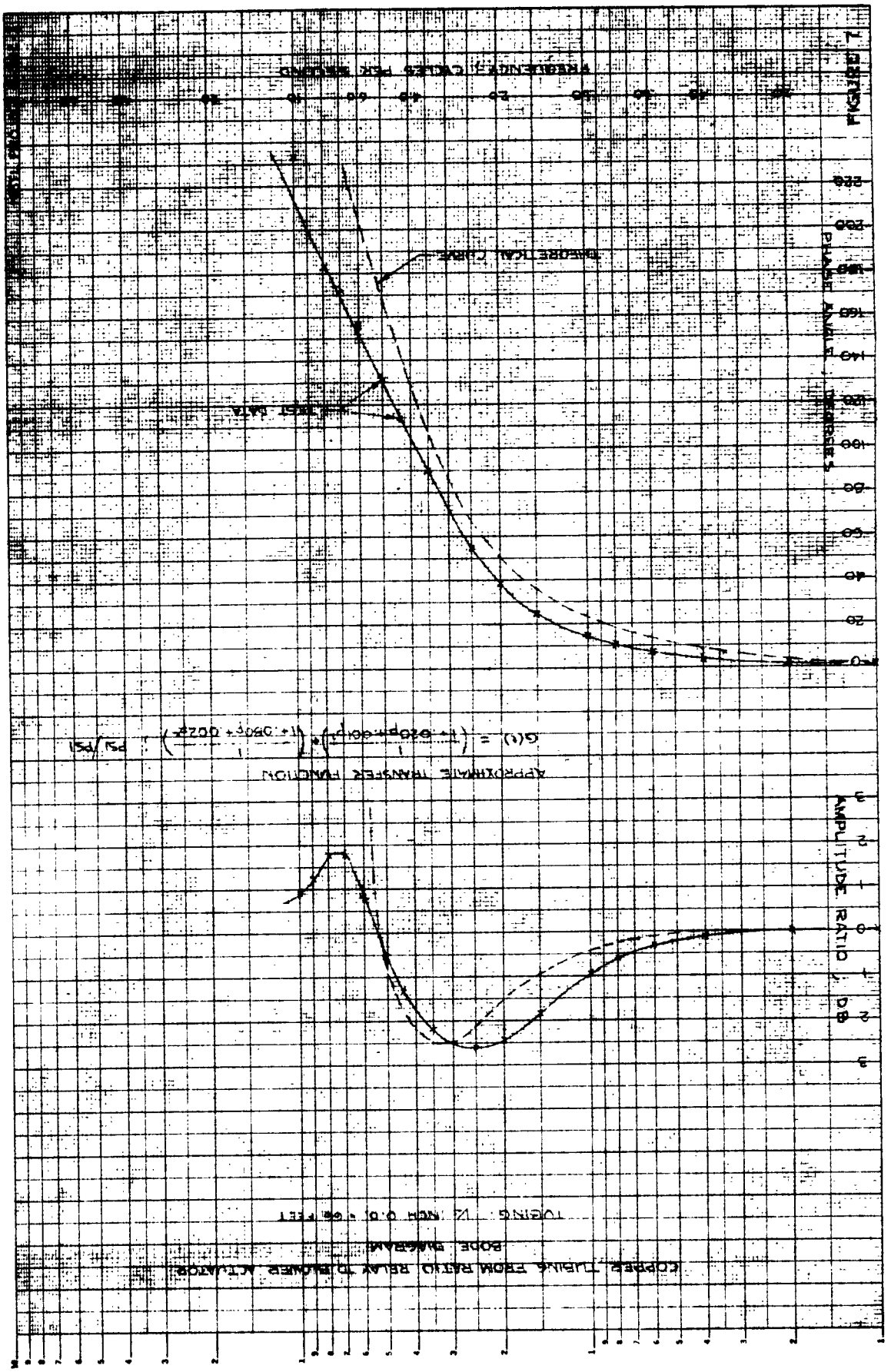
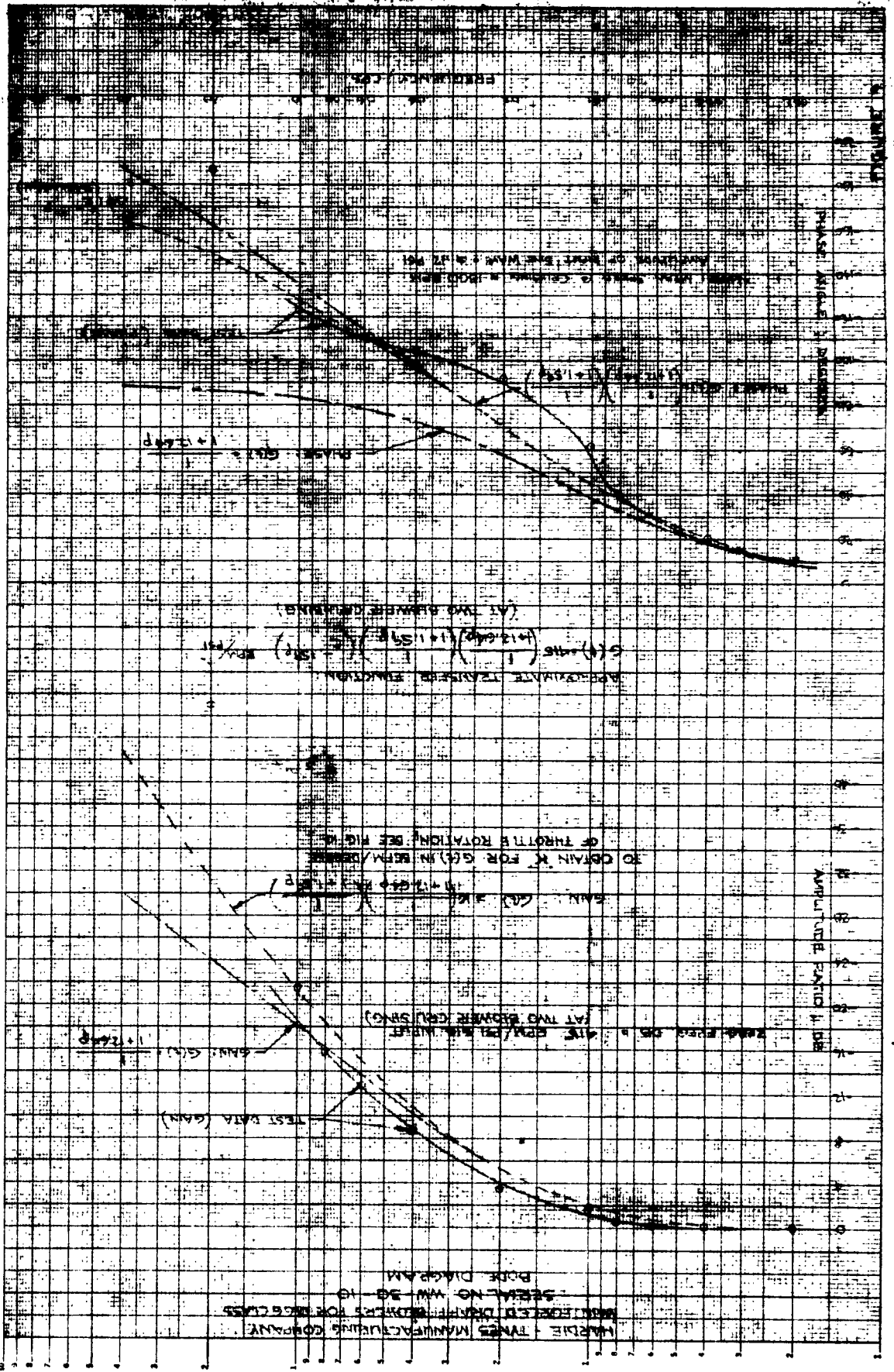
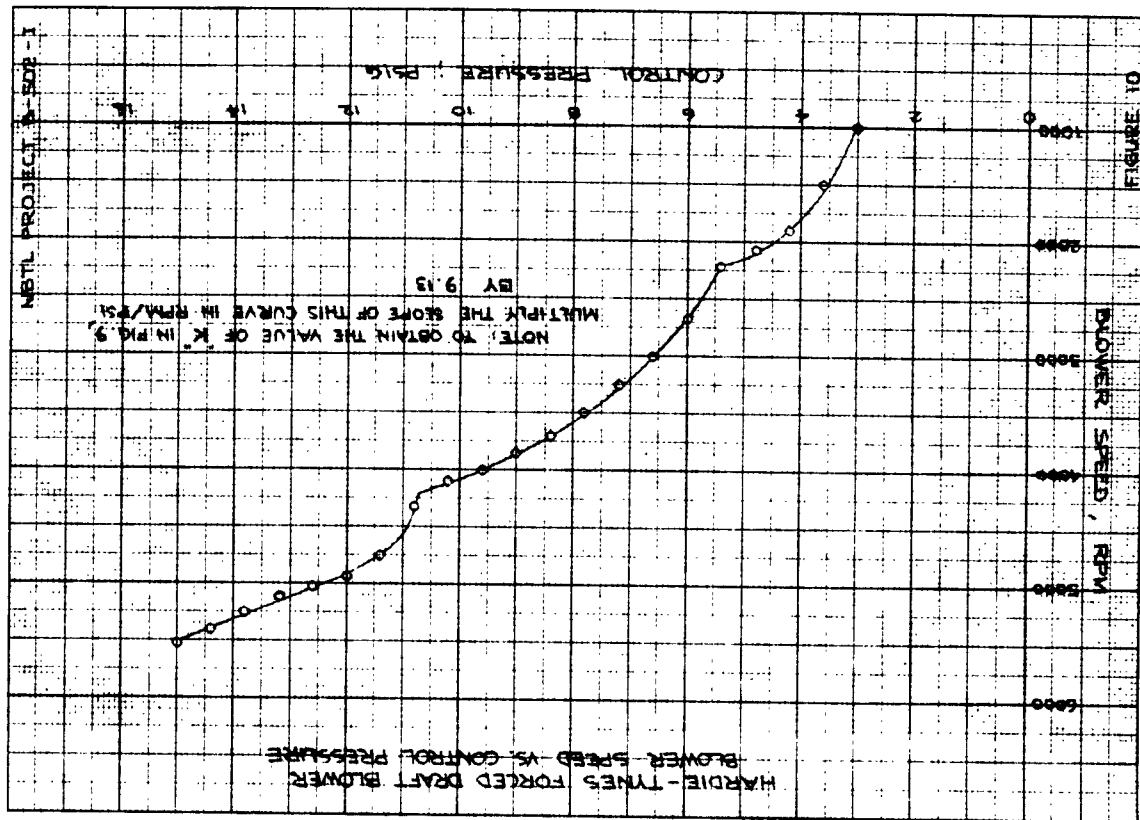


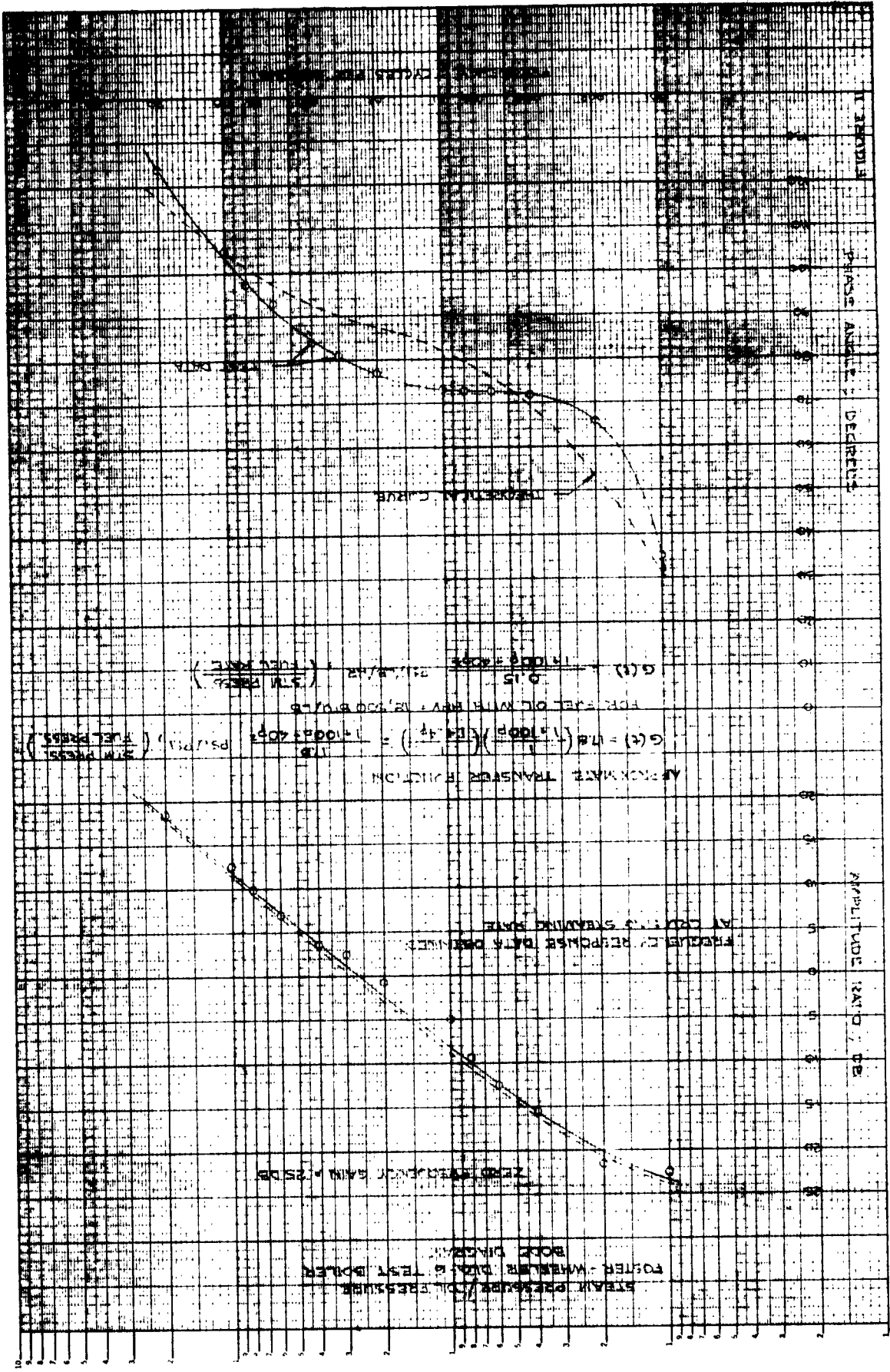
FIGURE 6











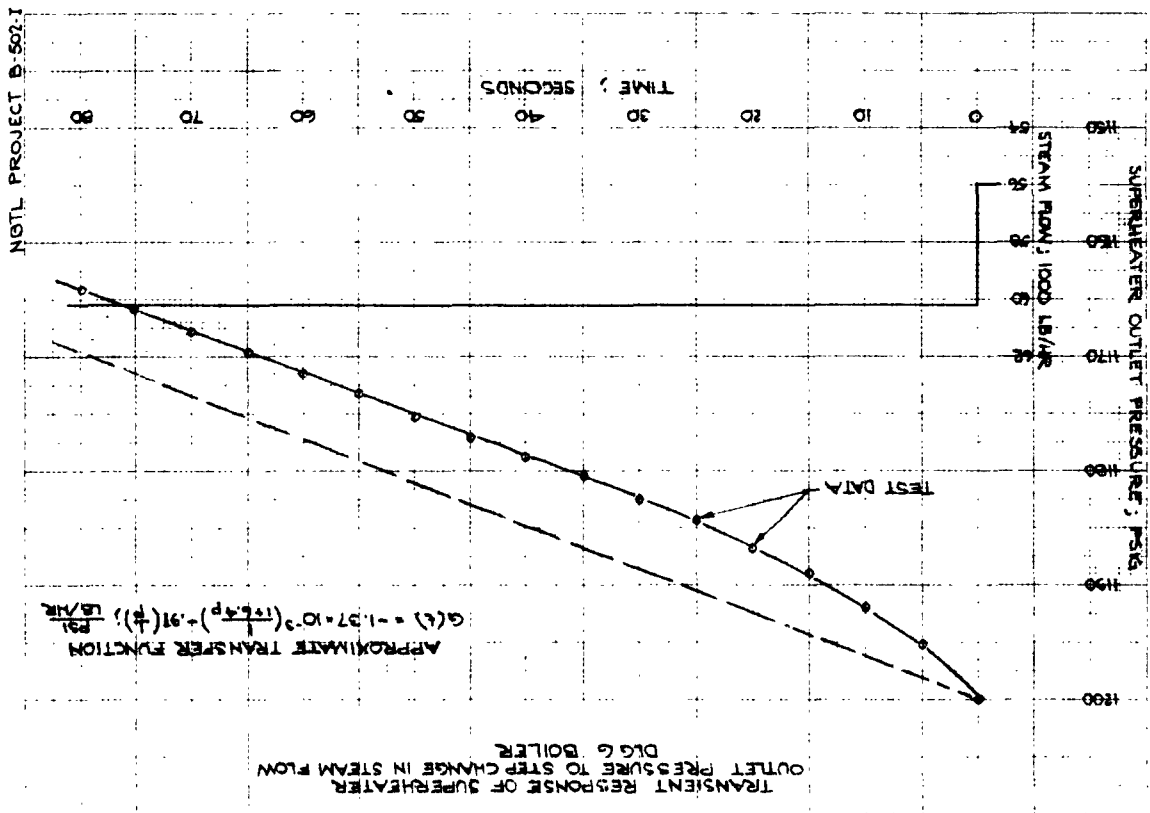


FIGURE 12

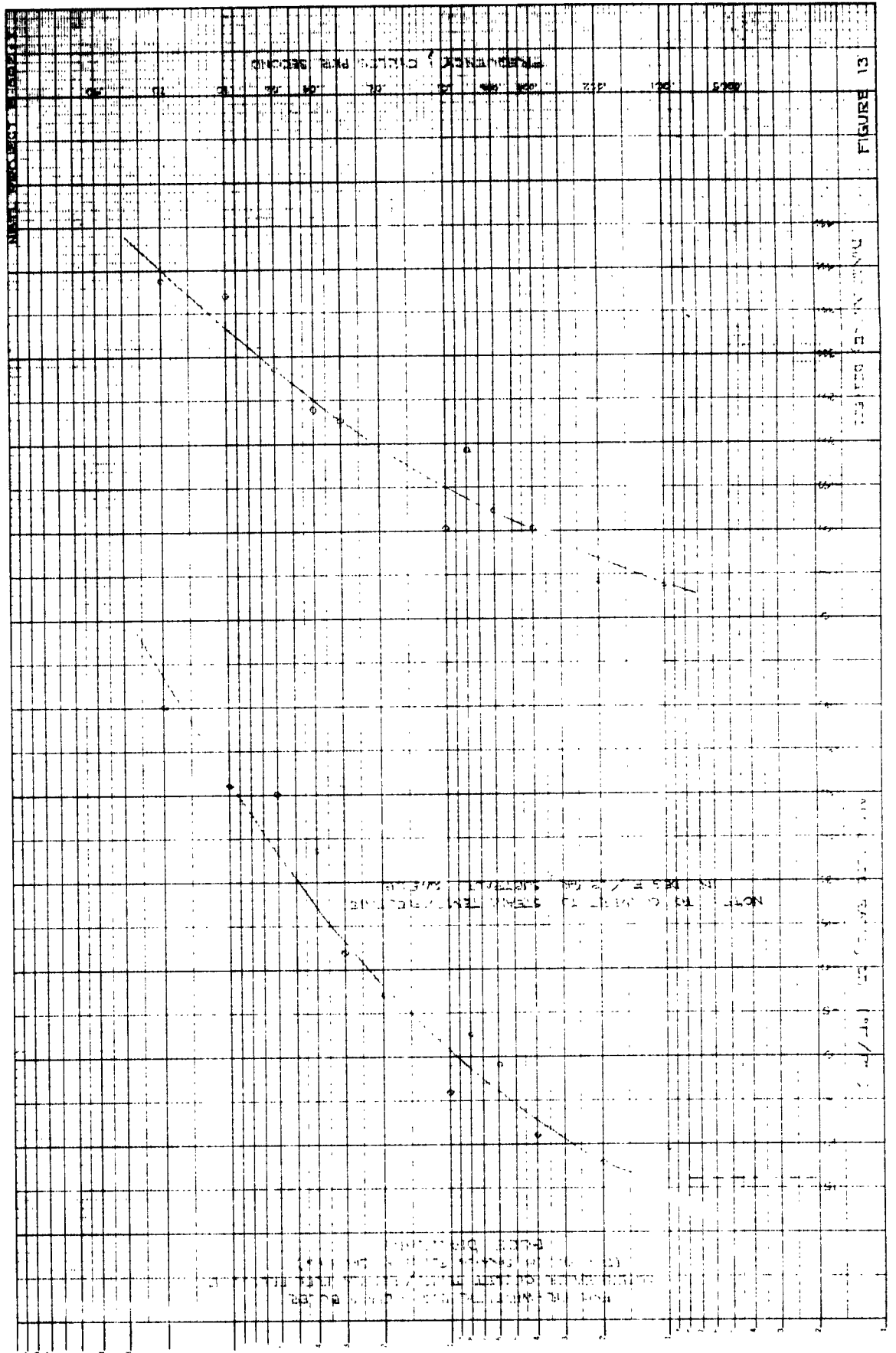


FIGURE 13

TEMPERATURE IN DEGREES CENTIGRADE

TEMPERATURE IN DEGREES CENTIGRADE

TEMPERATURE IN DEGREES CENTIGRADE

NOTE: THE TEMPERATURE IN DEGREES CENTIGRADE IS SHOWN ON THE Y-AXIS.

THE TEMPERATURE IN DEGREES CENTIGRADE IS SHOWN ON THE Y-AXIS.  
 THE TIME IN SECONDS IS SHOWN ON THE X-AXIS.  
 THE TEMPERATURE IN DEGREES CENTIGRADE IS SHOWN ON THE Y-AXIS.  
 THE TIME IN SECONDS IS SHOWN ON THE X-AXIS.

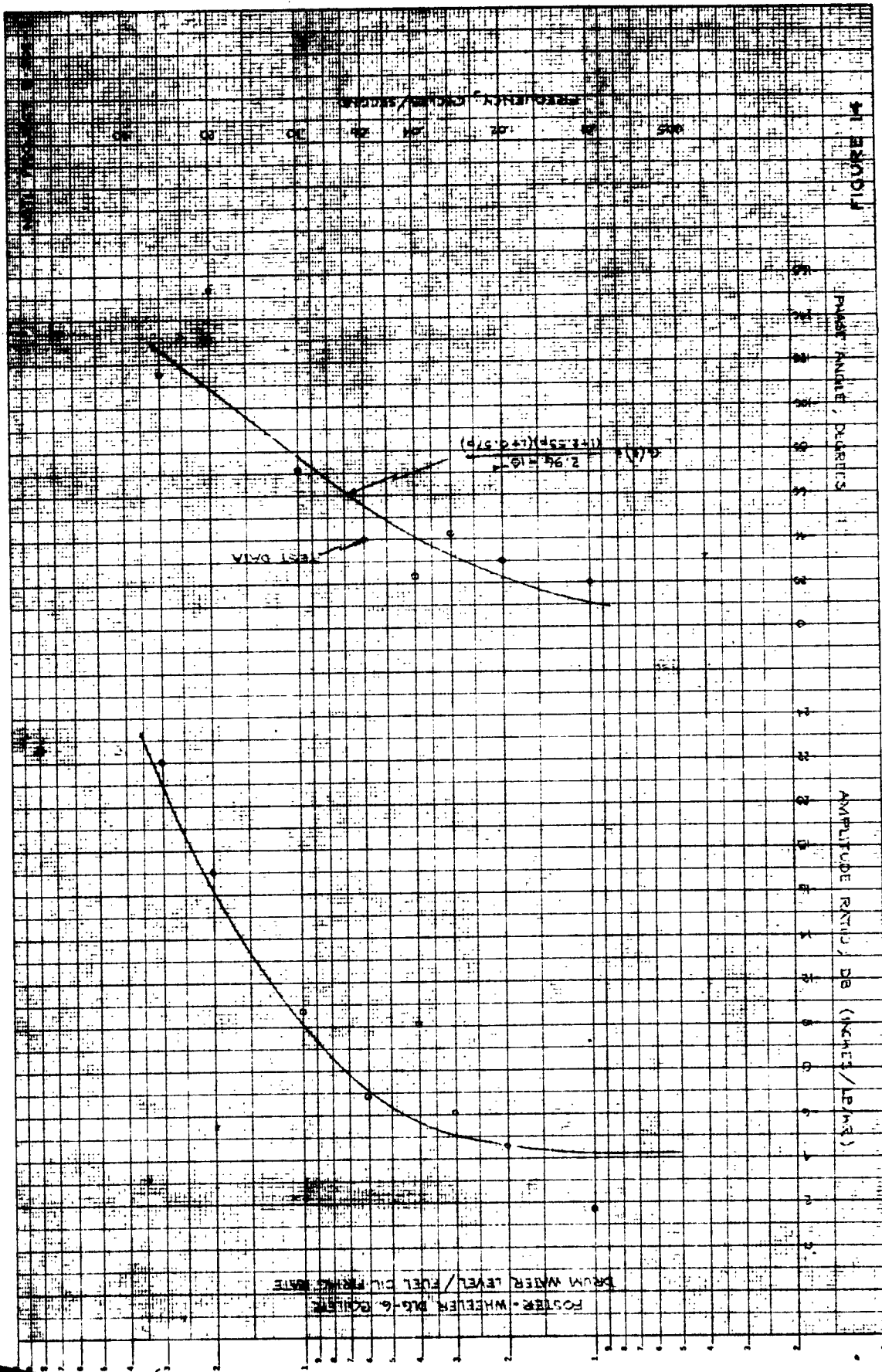
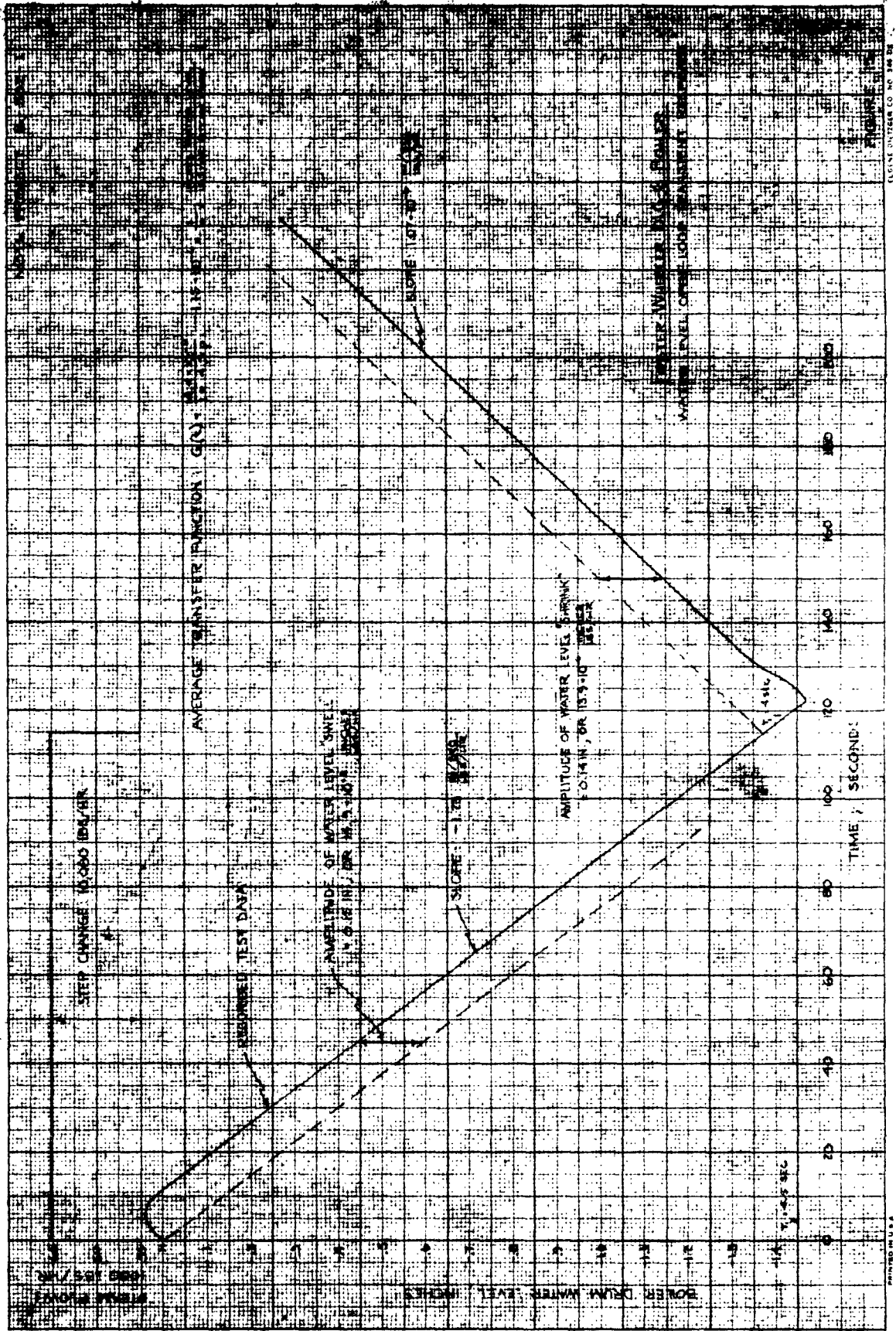
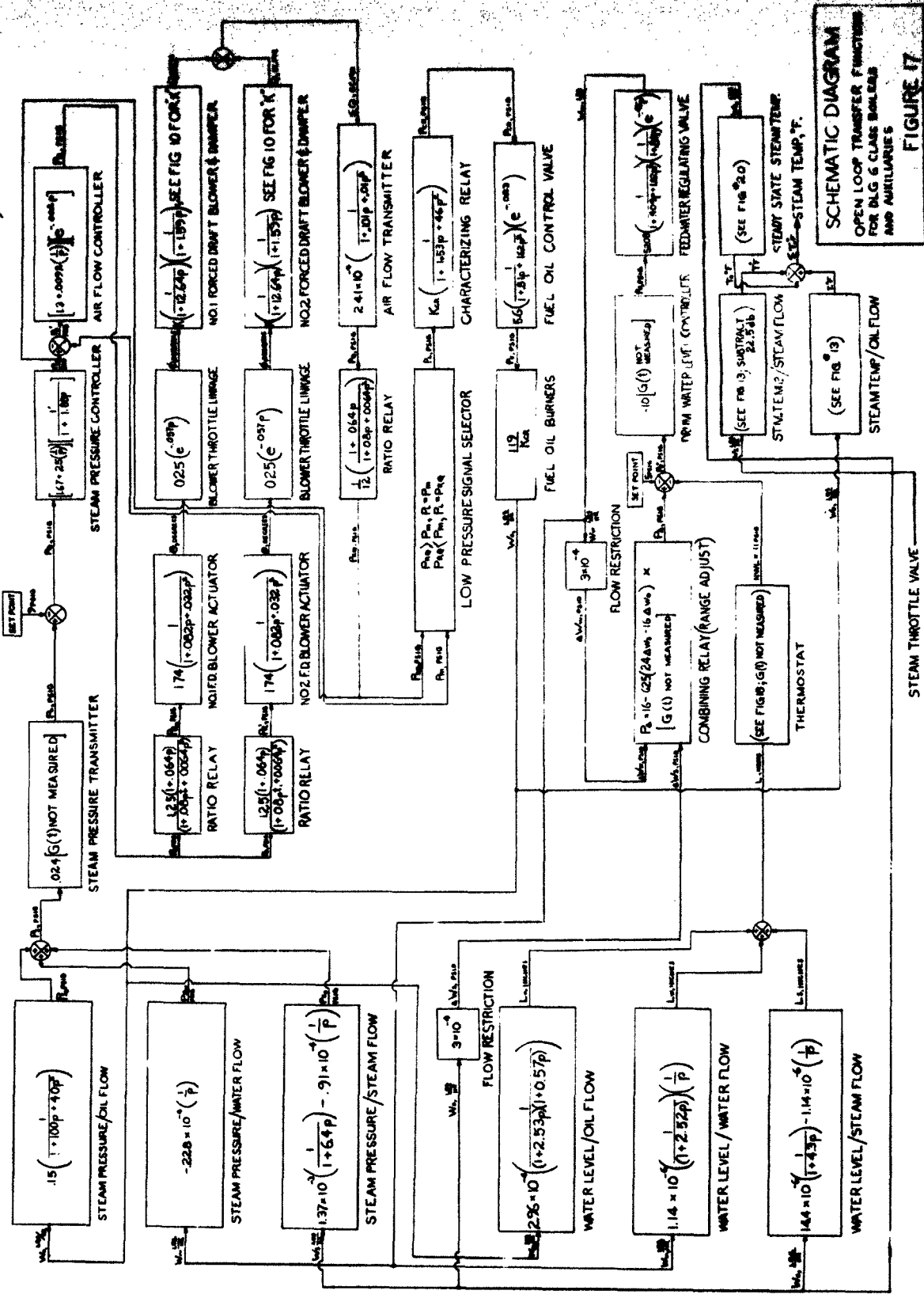


FIGURE 14





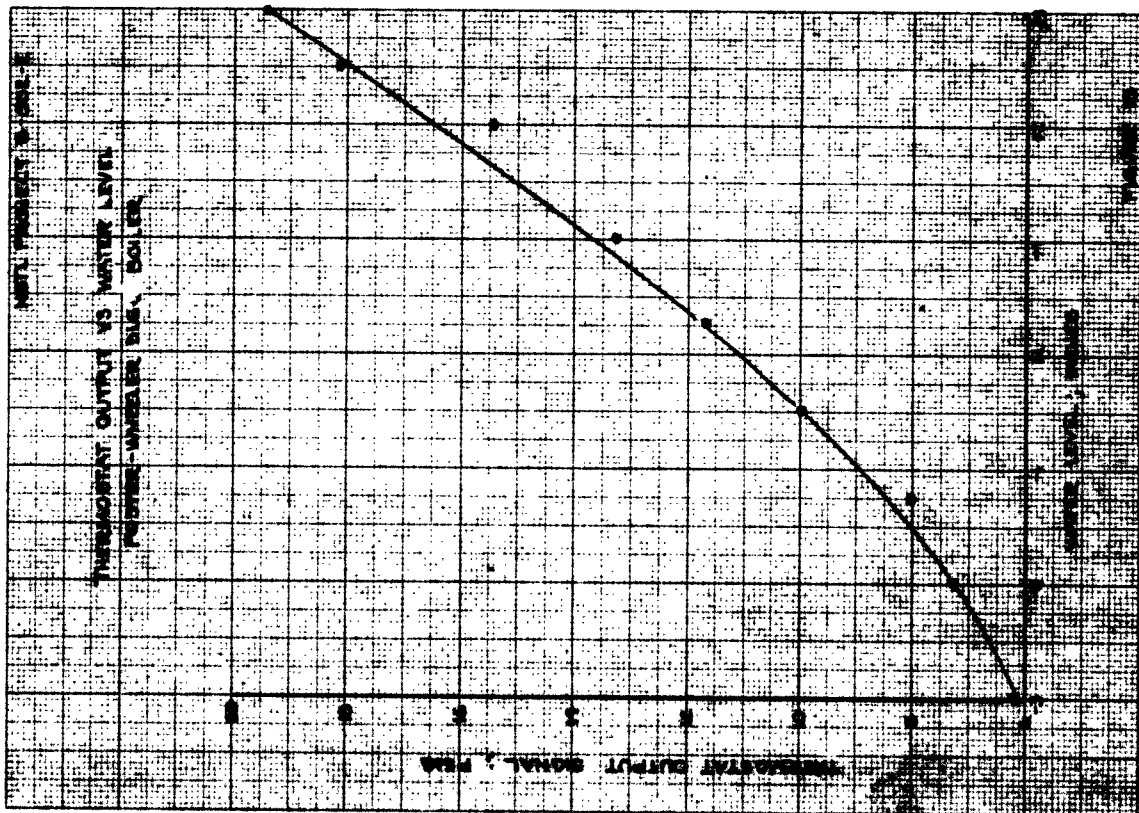
NBTL PROJECT B-503-1



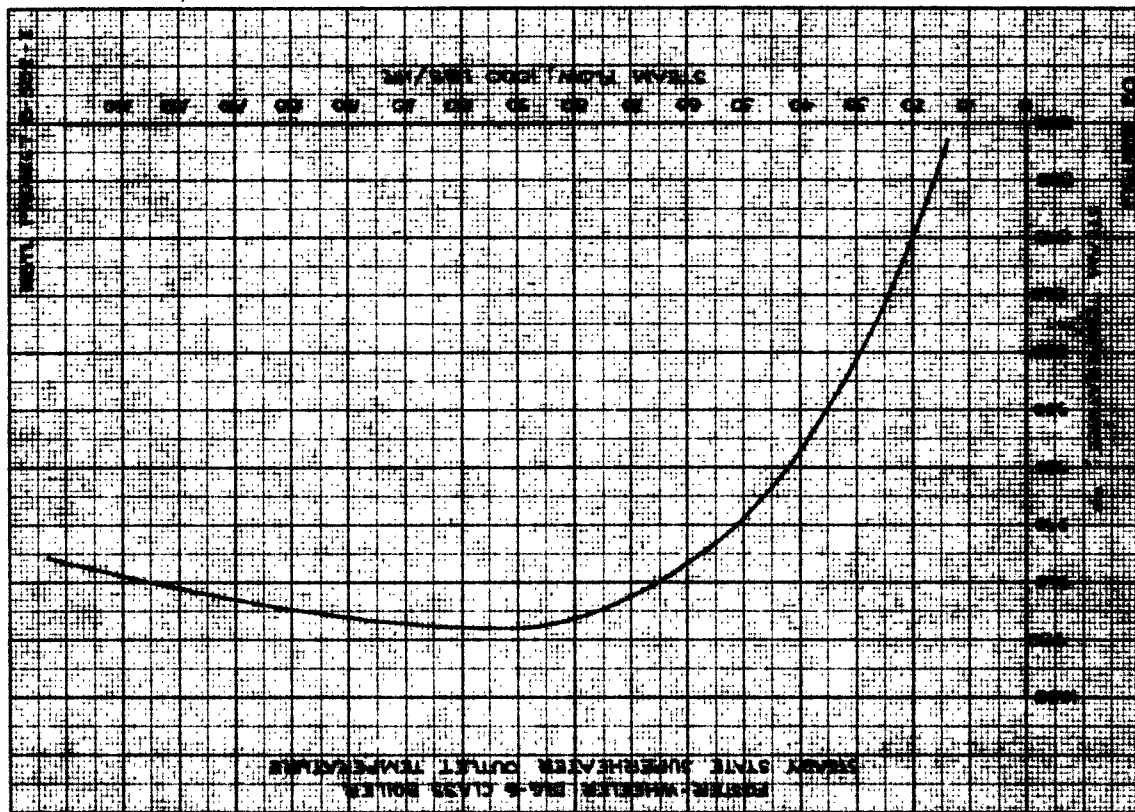
SCHEMATIC DIAGRAM  
OPEN LOOP TRANSFER FUNCTION  
FOR DLG & CLASS BOILER  
AND AUXILIARIES

FIGURE 17

STEAM THROTTLE VALVE







<p>Naval Boiler and Turbine Laboratory Project No. B-502-I EXPERIMENTAL DETERMINATION OF OPEN-LOOP FREQUENCY RESPONSE CHARACTERISTICS OF DLG-6 CLASS STEAM GENERATOR SYSTEM, by J. W. Banham, Jr. P. H. Zavod 4 March 1963 41 p., 17 illus. UNCLASSIFIED</p> <p>Open loop frequency response measurements were made of the elements comprising the Foster- (over)</p>	<p>Naval Boiler and Turbine Laboratory Project No. B-502-I EXPERIMENTAL DETERMINATION OF OPEN-LOOP FREQUENCY RESPONSE CHARACTERISTICS OF DLG-6 CLASS STEAM GENERATOR SYSTEM, by J. W. Banham, Jr. P. H. Zavod 4 March 1963 41 p., 17 illus. UNCLASSIFIED</p> <p>Open loop frequency response measurements were made of the elements comprising the Foster- (over)</p>	<p>I. Banham, J.W., Jr. Zavod, P.H. II. Foster-Wheeler Corp., General Regulator Corp., Copes-Vulcan Div., Hardie-Tynes Mfg. Co. III. DLG-6 Class IV. SF013-06-06 Task 4182</p> <p>UNCLASSIFIED</p>
<p>Naval Boiler and Turbine Laboratory Project No. B-502-I EXPERIMENTAL DETERMINATION OF OPEN-LOOP FREQUENCY RESPONSE CHARACTERISTICS OF DLG-6 CLASS STEAM GENERATOR SYSTEM, by J. W. Banham, Jr. P. H. Zavod 4 March 1963 41 p., 17 illus. UNCLASSIFIED</p> <p>Open loop frequency response measurements were made of the elements comprising the Foster- (over)</p>	<p>Naval Boiler and Turbine Laboratory Project No. B-502-I EXPERIMENTAL DETERMINATION OF OPEN-LOOP FREQUENCY RESPONSE CHARACTERISTICS OF DLG-6 CLASS STEAM GENERATOR SYSTEM, by J. W. Banham, Jr. P. H. Zavod 4 March 1963 41 p., 17 illus. UNCLASSIFIED</p> <p>Open loop frequency response measurements were made of the elements comprising the Foster- (over)</p>	<p>I. Banham, J.W., Jr. Zavod, P.H. II. Foster-Wheeler Corp., General Regulator Corp., Copes-Vulcan Div., Hardie-Tynes Mfg. Co. III. DLG-6 Class IV. SF013-06-06 Task 4182</p> <p>UNCLASSIFIED</p>

to large phase lags inherent in the process at low frequencies. The chief offenders in this regard are the forced draft blowers, the heat sink, and the additional integrations in the controllers themselves.

to large phase lags inherent in the process at low frequencies. The chief offenders in this regard are the forced draft blowers, the heat sink, and the additional integrations in the controllers themselves.

to large phase lags inherent in the process at low frequencies. The chief offenders in this regard are the forced draft blowers, the heat sink, and the additional integrations in the controllers themselves.

to large phase lags inherent in the process at low frequencies. The chief offenders in this regard are the forced draft blowers, the heat sink, and the additional integrations in the controllers themselves.